Archives of Biochemistry and Biophysics 577–578 (2015) 24–34

Contents lists available at ScienceDirect

Archives of Biochemistry and Biophysics

journal homepage: www.elsevier.com/locate/yabbi

Mechanistic studies of the tyrosinase-catalyzed oxidative cyclocondensation of 2-aminophenol to 2-aminophenoxazin-3-one

Courtney Washington [a], Jamere Maxwell [a], Joenathan Stevenson [a], Gregory Malone [a], Edward W. Lowe Jr. [b], Qiang Zhang [a], Guangdi Wang [a], Neil R. McIntyre [a,*]

[a] Division of Mathematical and Physical Sciences, Department of Chemistry, Xavier University of Louisiana, New Orleans, LA 70125, USA
[b] Center for Structural Biology, Vanderbilt University, Nashville, TN 37232, USA

ARTICLE INFO

Article history:
Received 6 January 2015
and in revised form 20 April 2015
Available online 14 May 2015

Keywords:
Isotope effect
Tyrosinase
2-Aminophenol
Mechanism
Cyclocondensation
Kinetics

ABSTRACT

Tyrosinase (EC 1.14.18.1) catalyzes the monophenolase and diphenolase reaction associated with vertebrate pigmentation and fruit/vegetable browning. Tyrosinase is an oxygen-dependent, dicopper enzyme that has three states: E_{met}, E_{oxy}, and E_{deoxy}. The diphenolase activity can be carried out by both the met and the oxy states of the enzyme while neither mono- nor diphenolase activity results from the *deoxy* state. In this study, the oxidative cyclocondensation of 2-aminophenol (OAP) to the corresponding 2-aminophenoxazin-3-one (APX) by mushroom tyrosinase was investigated. Using a combination of various steady- and pre-steady state methodologies, we have investigated the kinetic and chemical mechanism of this reaction. The k_{cat} for OAP is 75 ± 2 s^{-1}, K_M^{OAP} = 1.8 ± 0.2 mM, $K_M^{O_2}$ = 25 ± 4 μM with substrates binding in a steady-state preferred fashion. Stopped flow and global analysis support a model where OAP preferentially binds to the *oxy* form over the *met* ($k_7 \gg k_1$). For the *met* form, His269 and His61 are the proposed bases, while the *oxy* form uses the copper-peroxide and His61 for the sequential deprotonation of anilinic and phenolic hydrogens. Solvent KIEs show proton transfer to be increasingly rate limiting for k_{cat}/K_M^{OAP} as $[O_2] \rightarrow 0$ μM (1.38 ± 0.06) decreasing to 0.83 ± 0.03 as $[O_2] \rightarrow \infty$ reflecting a partially rate limiting μ-OH bond cleavage (E_{met}) and formation (E_{oxy}) following protonation in the transition state. The coupling and cyclization reactions of *o*-quinone imine and OAP pass through a phenyl*imino*cyclohexadione intermediate to APX, forming at a rate of 6.91 ± 0.03 $\mu M^{-1}s^{-1}$ and 2.59E−2 ± 5.31E−4 s^{-1}. Differences in reactivity attributed to the anilinic moiety of OAP with *o*-diphenols are discussed.

Introduction

Tyrosinase (E.C. 1.14.18.1) is a member of the type-3 copper protein family catalyzing the monophenolase and diphenolase activity on phenolic/anilinic and catechol, 2-aminophenol and 2-aminoaniline substrates, respectively [1–6]. Representative members of the type-3 copper protein family include: catechol oxidase (CO), hemocyanin (Hc) and tyrosinase (Ty) though members have diverse functions. Tyrosinase is associated with pigmentation catalyzing the first step in melanin biosynthesis – a pigment ubiquitously present in all phyla [6]. The structure of mushroom (*Agaricus bisporus*) tyrosinase (abTy) is a tetrameric protein with 2 heavy (H, 392 aa, ~43 kDa) and 2 light (L, 150 aa, ~14 kDa) chains (2.30 Å resolution, 2Y9W) [7,8]. As a derivative of the *ppo3* gene, the fungal enzyme is structurally homologous to other tyrosinases, only larger with 110 more residues present as loops connecting conserved secondary structural elements. H-subunits of abTy contain 13 α-helices, 8 mostly short β-strands and many loops, similar to known type-3 protein structures including: tyrosinase structures from *Streptomyces castaneoglobisporus* [9] and *Bacillus megaterium* [10,11] as well as *Octopus dolfeini* Hc [12] and *Ipomoea batatas* catechol oxidase [13]. Within the H-subunit, the dicopper binding domain is comprised of four antiparallel helices (α3, α4, and α10, α11) positioned perpendicularly with CuA is coordinated by H61 (α3), H94 (α4) and H85 (loop connecting α3 to α4) and CuB by H259, H263 (α10) and H296 (α11). The structure of the L-subunit in abTy is best described as a β-trefoil fold with 12 antiparallel β-strands assembled in a cylindrical barrel of six 2-stranded sheets [7]. The L-subunit appears to play a structural role in tetramer formation positioned 25 Å away from the active site as H-subunit turnover number is unaffected by its absence.

The di-copper domain in tyrosinase is classified by three distinct geometric and electronic architectures with alternate function

* Corresponding author.
E-mail address: nmcintyr@xula.edu (N.R. McIntyre).

http://dx.doi.org/10.1016/j.abb.2015.04.007
0003-9861/

toward substrate oxidation: E_{deoxy}, E_{met}, and E_{oxy} in addition to an inactive mixed valent copper form [14]. The *oxy*-state (E_{oxy}) of tyrosinase has molecular oxygen bound in a side-on $\mu-\eta^2{:}\eta^2$ geometry linked to the solvent-bridged *met*-state (μ-OH) and the reduced *deoxy*-state through the reversible exchange of the ligand as oxygen (E_{deoxy}) or peroxide (E_{met}) [15]. The mechanism for tyrosinase-catalyzed phenol (monophenolase) and *o*-diphenol (diphenolase) oxidation has been investigated using steady-state, transient phase and kinetic isotope effects [16–22]. The monophenolase (monooxygenase) activity is catalyzed by tyrosinase in the E_{oxy} form while the *o*-diphenolase (oxidase) activity results from both E_{met} and E_{oxy} forms of the enzyme [19]. Several tyrosinase studies demonstrate that the E_{oxy} form is stable and subsequently reduced to E_{met} with the concomitant oxidation of *o*-diphenol to the corresponding *o*-quinone [23–25]. Evaluation of the abTy *o*-diphenolase reaction mechanism demonstrate tight O_2 binding in addition to an increased second-order rate constant for the *o*-diphenol substrate to preferentially bind with the E_{met} state over the E_{oxy} form of the enzyme [20]. The monophenolase activity of tyrosinase utilizes an electrophilic aromatic substitution (EAS) mechanism for *ortho*-hydroxylation.

Interestingly, tyrosinase and type-3 model complexes lack an observable kinetic isotope effect (KIE) with *ortho*-deuterated monophenol substrates. This suggests that the *ortho*-deprotonation step in this mechanism is either extremely slow or concerted with the oxygen insertion step. The observation of a normal KIE (>1) was revealed upon deuteration of the phenolic hydrogen for both phenol and *o*-diphenol substrates [16,17,26,27]. With proton inventory solvent KIE (sKIE) studies, the mechanism for monophenolase and diphenolase tyrosinase activity support a partially-rate limiting proton transfer in both E_{met} and E_{oxy} forms attributed to nucleophilic attack by the corresponding phenolate ion to copper [16,17].

Structure–function relationships illustrate drastically altered sKIE values based on the para substituent of the substrate. Therein, the fractionation factors (ϕ) decrease as the observed sKIE for k_{cat} increase with each mode of abTy-dependent oxidation. For monophenolase activity, the lowest fractionation factor values and highest sKIE were observed for substrates with an ionic para substituent. For diphenolase activity, the trend is less clear coupling higher fractionation factors with lower sKIE values compared to those reported for the monophenolase reaction. These finding are consistent with a general base catalytic mechanism important to deprotonate substrate phenolic hydrogens that contribute to the stabilization of slightly altered transition state geometries from either the E_{oxy} or E_{met} reaction coordinates [28–34]. The extent of transition state stabilization through altered protonic interactions support the presence of a far different microenvironment for the diphenolase reaction coordinate compared to that observed for monophenolase activity.

The precedence for 2-aminophenol oxidase activity has been previously observed in several copper containing enzymes (laccase [36], tyrosinase [1] and various homologues such as: griF [37], phenoxazinone synthase [38]) as well as biomimetic complexes ranging from copper through manganese [39]. The oxidation of 2-aminophenols by tyrosinase has been previously studied showing a mechanism similar to catechol compounds [2]. For *o*-aminophenol oxidation, the turnover number is decreased relative to the *o* -diphenol substrates though K_M values does not appear to be dramatically affected by the structural difference [1]. The resulting *o*-quinone imine (Q) undergoes a sequential coupling and cyclization towards the corresponding planar 2-3*H*-aminophenoxazin-3-one (APX) structure passing through several proposed intermediates (Scheme 1) [35,40]. Our current study of 2-aminophenol oxidation by abTy was performed to increase the present body of data contrasting the oxidase mechanism for 2-aminophenol with *o*-diphenol. The role of the phenylamine moiety was studied using a mixture of steady-state and transient phase kinetics, sKIEs, global analysis and molecular modeling studies to characterize multiple aspects of the enzymatic and non-enzymatic reaction coordinate for 2-aminophenol oxidation. Therein, we present experimental evidence supporting a distinct preference for 2-aminophenol oxidation by the E_{oxy} form of abTy (over the more stable E_{met} form) to produce the *o*-quinone imine product which passes through a spectroscopically observed transient phenyliminocyclodione intermediate prior to APX product formation.

Materials and methods

Reagents

Mushroom tyrosinase (3300 U/mg), 2-aminophenol, L-ascorbic acid, D_2O, mono-, di- and tri-sodium phosphate, DMSO, DMSO-d_6 and purchased from Sigma–Aldrich Co. (St. Louis, MO). HPLC-grade solvents (acetonitrile, methanol, and water) were purchased from Fisher Scientific (Fair Lawn, NJ). Analytical standards were purchased from Sigma–Aldrich Co. (St. Louis, MO). All other experimental reagents were purchased from commercial sources at highest purity grade available and used without additional modification. Commercial enzyme was purified following the procedure of Duckworth and Coleman [41] or the IMAC method [42]. Protein concentration was determined by the bicinchoninic acid assay [43] with bovine serum albumin as standard. Protein purity was assessed by sodium dodecyl sulfate–polyacrylamide gel electrophoresis.

Oxygen electrode

Reactions at 37.0 ± 0.1 °C were initiated by the addition of ~0.10–0.50 μM mushroom tyrosinase (4–5 μL) into 2.0 mL of 100 mM sodium phosphate (pH 6.4). Initial velocities were measured at varying concentrations of 2-aminophenol and oxygen. Initial rates were measured by following the tyrosinase-dependent consumption of O_2 using a Yellow Springs Instrument Model 5300 oxygen monitor interfaced with a personal computer using a Dataq Instruments analogue/digital converter (model DI-158RS) interfaced to Microsoft Excel through the Windaq module, modified from McIntyre et al. [44]. Using a Maxtec Low flow oxygen blender, *in situ* [O_2] was changed by varying the percent mixtures

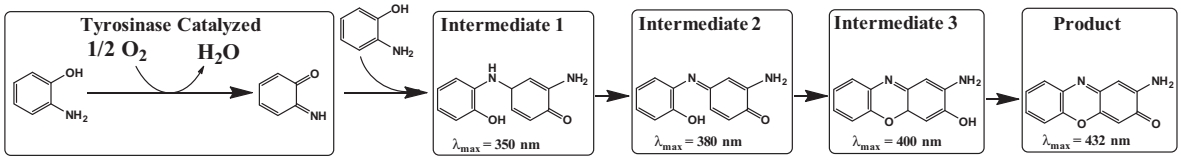

Scheme 1. Reaction stoichiometry for the tyrosinase catalyzed oxidation of 2-aminophenol to *o*-quinone imine followed by *non-enzymatic* coupling with 2-aminophenol passing through several proposed intermediate structures to give 2-amino-3*H*-phenoxazin-3-one (product). Please note, estimates for the λ_{max} for intermediates were based on previous work by Barry et al. [35].